

# Lab on a Chip

Accepted Manuscript



This is an *Accepted Manuscript*, which has been through the Royal Society of Chemistry peer review process and has been accepted for publication.

*Accepted Manuscripts* are published online shortly after acceptance, before technical editing, formatting and proof reading. Using this free service, authors can make their results available to the community, in citable form, before we publish the edited article. We will replace this *Accepted Manuscript* with the edited and formatted *Advance Article* as soon as it is available.

You can find more information about *Accepted Manuscripts* in the [Information for Authors](#).

Please note that technical editing may introduce minor changes to the text and/or graphics, which may alter content. The journal's standard [Terms & Conditions](#) and the [Ethical guidelines](#) still apply. In no event shall the Royal Society of Chemistry be held responsible for any errors or omissions in this *Accepted Manuscript* or any consequences arising from the use of any information it contains.

## ARTICLE

# Three-dimensional heterogeneous assembly of coded microgels using an untethered mobile microgripper

Cite this: DOI: 10.1039/x0xx00000x

Su Eun Chung<sup>at</sup>, Xiaoguang Dong<sup>at</sup>, and Metin Sitti<sup>a,b</sup>Received 00th January 2012,  
Accepted 00th January 2012

DOI: 10.1039/x0xx00000x

[www.rsc.org/](http://www.rsc.org/)

Three-dimensional (3D) heterogeneous assembly of coded microgels in enclosed aquatic environments is demonstrated using a remotely actuated and controlled magnetic microgripper by a customized electromagnetic coil system. The microgripper uses different 'stick-slip' and 'rolling' locomotion in 2D and also levitation in 3D by magnetic gradient-based pulling force. This enables the microrobot to precisely manipulate each microgel by controlling its position and orientation in all *x-y-z* directions. Our microrobotic assembly method broke the barrier of limitation on the number of assembled microgel layers, because it enabled precise 3D levitation of the microgripper. We used the gripper to assemble microgels that had been coded with different colours and shapes onto prefabricated polymeric microposts. This eliminates the need for extra secondary cross-linking to fix the final construct. We demonstrated assembly of microgels on a single micropost up to ten layers. By increasing the number and changing the distribution of the posts, complex heterogeneous microsystems were possible to construct in 3D.

## Introduction

Microgels are soft tissue-like hydrogels used for a significant amount of biomedical applications due to their similarity with extracellular matrix and hydrophilic characteristics.<sup>1,2</sup> Various kinds of biological materials, such as mammalian cells, can be encapsulated inside microgels to mimic three-dimensional (3D) tissue constructs by assembling the microgels as unit building blocks.<sup>3</sup> 3D tissue constructs are important to study how cells or tissues function as parts of living organs rather than two-dimensional (2D) cell-culture models. Many researchers have been studying how to manipulate and assemble these microgel blocks with many different techniques to construct 3D cell culture scaffolds. Building up 3D constructs with cell-encapsulated small microgel building blocks is more advantageous than spreading cells into prefabricated 3D scaffolds.<sup>4</sup> Cells can be distributed homogeneously within the whole structure and assembly method provides flexibility to build larger-size complex tissue constructs with heterogeneous and different shape microgel building blocks.

Self-assembly is a parallel and fast assembly method, which transports components to specified assembly sites with proper driving forces at the equilibrium state. Most of the existing microgel assembly methods are based on self-assembly approaches. Capillary force based assembly, which minimizes surface free energy, is a very fast process, but assembling a desired asymmetric complex 3D construct is hard to realize with a non-directed self-assembly.<sup>5,6</sup> Instead of a confined chamber, flowing liquid in a microfluidic channel could assist microgels to be self-assembled directionally in 3D, but the direction and the format of the assembly mostly depend on the direction of flow, causing mainly one-dimensional (1D)

constructs.<sup>7,8</sup> In addition, electrostatic interaction forces,<sup>9</sup> acoustic waves,<sup>10</sup> or magnetic forces<sup>11,12</sup> can also direct the self-assembly of microgels in 3D. However, because the position, direction, and orientation of each microgel is not controlled individually, self-assembly methods cannot precisely control the number and layers of microgels during the process forming final 3D construct.

In contrast, robotic assembly can control the position and orientation of individual microgels during the assembly process. Teams of micromanipulators were used to assemble microgels to mimic vascular-like tissues by inserting their tips into donut-shaped microgels.<sup>13</sup> In this method, all the robots were directly connected to the stepping motor and only moved along the rail. This was better than manual assembly of microgels<sup>14</sup> or self-assembly methods to construct 3D shapes, but the robots could only work in open channels, not enclosed microfluidic or other environments such as inside the human body. Recently developed microrobots<sup>15-18</sup>, which are remotely controlled by an electromagnetic coil system, could directly push microgels and assemble them into complex structures in enclosed spaces.<sup>19</sup> However, the microrobots in such studies could only move the microgels by pushing on a substrate in 2D to create 3D structures with assistance of ramps and plateaus. Therefore, it was hard to precisely assemble microgels more than three layers. To create out-of-plane complex 3D assembly precisely and flexibly, an untethered magnetic microgripper was introduced to directly pick-and-place an object.<sup>20</sup> However, the gripper could still only use 'stick-slip' and 'rolling' 2D locomotion to conduct pick-and-place. Thus, the length of the gripper limited the maximum vertical target position of the object to be assembled, e.g. the maximum number of layers of microgels to be assembled. Therefore, it has not yet been able

to construct more than three layers of microgels in enclosed spaces.

In this paper, we demonstrated 3D heterogeneous pick-and-place robotic assembly of microgels up to ten layers, targeting the application of engineering tissue reconstructions with 3D cell culture scaffolds in enclosed spaces, such as the human body. The mobile microgripper, remotely actuated and controlled by a customized electromagnetic coil system, was used to pick-and-place individual microgels to the target assembly site in aquatic environments. The microgripper uses different ‘stick-slip’ and ‘rolling’ locomotion in 2D and also levitation in 3D by magnetic gradient-based pulling force. This enables precise manipulation of each microgel by controlling the position and orientation of the microgel in all  $x$ - $y$ - $z$  directions. Our assembly method broke the barrier of limitation on the number of assembled microgel layers, because it enabled precise 3D levitation of the microgripper. With the assistance of prefabricated polymeric posts on the substrate, microgels coded with different shapes and colours were heterogeneously assembled on posts to ensure stability in enclosed aquatic environments. This eliminates the need for extra secondary cross-linking to fix the final construct. We demonstrated assembly of microgels on a single post up to ten layers. By simply increasing the number and changing the distribution of the posts, complex 3D heterogeneous constructs were also easily fabricated.

## Experimental Results

### Overall schematics

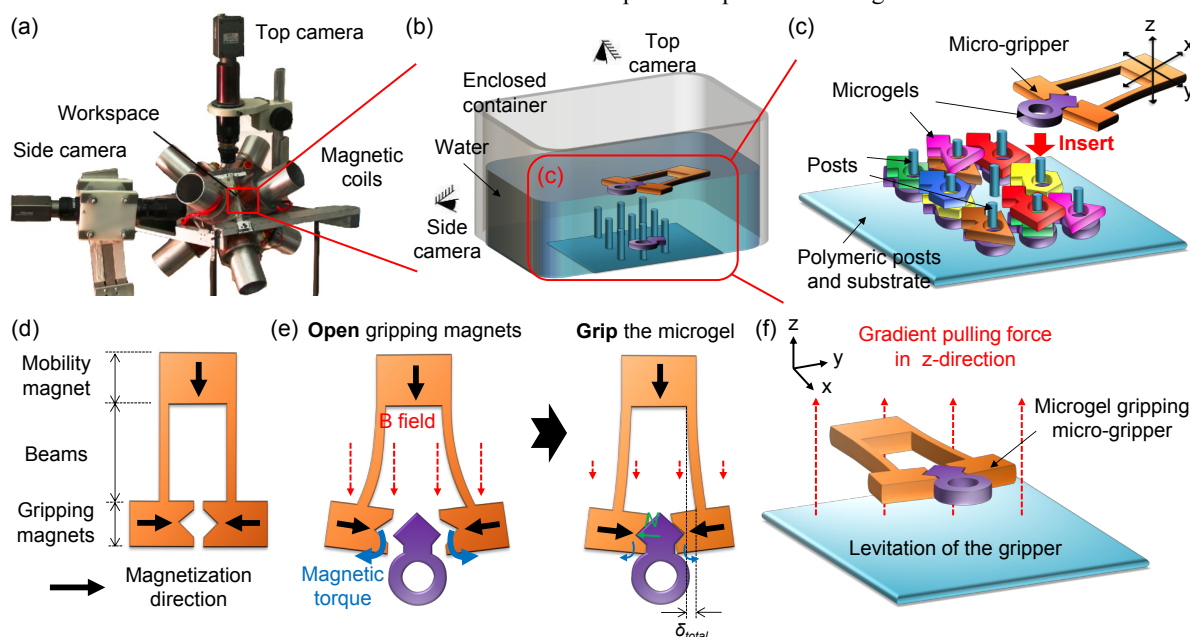


Figure 1 Schematic diagram of the 3D microgel assembly by a remotely controlled microgripper. (a) An electromagnetic coil system with eight coils was used to remotely actuate and control the microgripper. Two cameras were set up to observe the top view and the side view of the experimental workspace and localize the microgripper by using visual tracking during heterogeneous microgel assembly; (b) Experimental environments used for the microgel assembly: All the assembly process took place in a transparent container filled with deionized (DI) water; (c) Overall schematic diagram of the post-assisted 3D microgel assembly method: Various shape and colour coded microgels were heterogeneously assembled on the multiple posts to build 3D constructs in a stable manner by the microgripper; (d) Microgripper consisted of three parts: mobility magnet to move the gripper, beams which are flexures to be deflected when applying large magnetic field, and gripping magnets which work to open and close to grab the microgels. All the magnetization directions for each component were differently designed to actuate microgripper under applied magnetic field; (e) Microgripper actuation mechanism in 2D: The scheme of gripping was torque-based actuation. The gripping magnets with opposite magnetization directions were opened to grab the microgel due to applied

Figure 1 describes the experimental setup and schematic diagram of the 3D microgel robotic assembly mechanism using a remotely controlled mobile microgripper. The gripper was actuated and controlled by an electromagnetic coil system, composed of eight magnetic coils pointing to a centre workspace (Figure 1(a)). Two cameras were used to observe both the top view and the side view of the experimental workspace during localization of the gripper and 3D construction of microgels using the gripper. The whole assembly process took place in an aquatic environment, an enclosed transparent container filled with deionized (DI) water, as shown in Figure 1(b). Here, the gripper was remotely controlled in the enclosed workspace to assemble microgels, which has a potential to be used inside the human body for a biomedical application in the future. The gripper individually gripped, transported, and assembled the microgels on the assembly site. The prefabricated biocompatible polymeric substrate had multiple posts on top, and each microgel was put on the posts through a hole at the centre of the microgel (Figure 1(c)). The posts were used to fix the microgels during and after the assembly to create stable 3D structures. Therefore, the assembled structures will not move away from the target position or collapse due to liquid flow or other external disturbances. Various shape and colour coded microgels were heterogeneously assembled on multiple posts to build 3D constructs by the remotely controlled microgripper. Since the gripper could precisely manipulate an individual microgel dynamically, 3D patterns of heterogeneous assembly, such as number of microgel layers and composition of differently coded microgels on the post, could be easily controlled. Although the whole gripper was made out of the same composite magnetic material, each part worked with different functions to achieve pick-and-place of microgels.

magnetic torques, and closed to hold the microgel by reducing the magnetic field. In microgel-holding state, the total beam deflection  $\delta_{total}$  was defined as the distance between initial beam position and the deflected position due to holding microgel and affected by normal force  $N$  of the microgel. (f) Magnetic gradient pulling of microgripper in z-direction. Microgel-holding gripper with its gripping magnets was levitated from the substrate using magnetic gradient-based pulling in liquid environments.

As shown in Figure 1(d), the gripper was composed of three different parts: mobility magnet, thin beams, and gripping magnets. The mobility magnet dominated transitional movement of the gripper in the 2D plane and levitation of the gripper in the 3D space by magnetic gradient based pulling force. Two beams of the gripper were flexures, which contributed to the deflection of the gripper, and the final gap distance between gripping magnets was linearly proportional to the deflection of beams assuming small deflections. The gripping magnets were opened and closed to grab the microgels in 2D. The magnetization directions of each component were differently designed so that the microgripper could achieve both desired 2D and 3D locomotion and the function of opening and closing under an applied external magnetic field. The gripping magnets were designed to have opposite magnetization directions to each other, and they could be opened or closed to grab the microgel with applied magnetic torques.<sup>20</sup> Figures 1(e)-(f) show basic actuating mechanisms of a microgel pick-and-place by a microgripper. With an external magnetic field applied in the workspace, the gripping magnets experienced magnetic torques in opposite directions and the thin beams were bent in an outward direction. The deflection of the thin beams could be controlled precisely by applying different magnetic fields. First, the gripping magnets were opened larger than the microgel size, then they were controlled to close to hold the microgel by reducing the magnetic field. In contrast to the microgel gripping process, which took place

in 2D, transportation and assembly of microgels were completed in 3D. After gripping, the microgel-holding gripper was levitated from the substrate and moved to the target position by applying a magnetic gradient pulling force to the gripper. With these magnetic pick-and-place and heterogeneous assembly abilities in 3D, we could overcome the limitations of both current self-assembly and robotic assembly techniques.

To achieve the capability of picking-and-placing and assembling microgels in 3D, the grippers were designed to have proper beam deflecting ability to be able to pick and release the given size and shape of a microgel and to be easily levitated by the magnetic gradient pulling force. More details are included in '3D Magnetic Motion Control' of the Materials and Methods Section and 'Gripping Characterization and Analysis' in the Supplementary Information.

### Fabrication of microgels and polymeric posts

All the components used in the heterogeneous 3D assembly process were basically fabricated by a replica molding process to produce the fine shapes of the structures as shown in Figure 2. For negative rubber molds of both microgels and the microgripper, we casted silicon rubber over the patterned photoresist layer (Figure 2(a)).

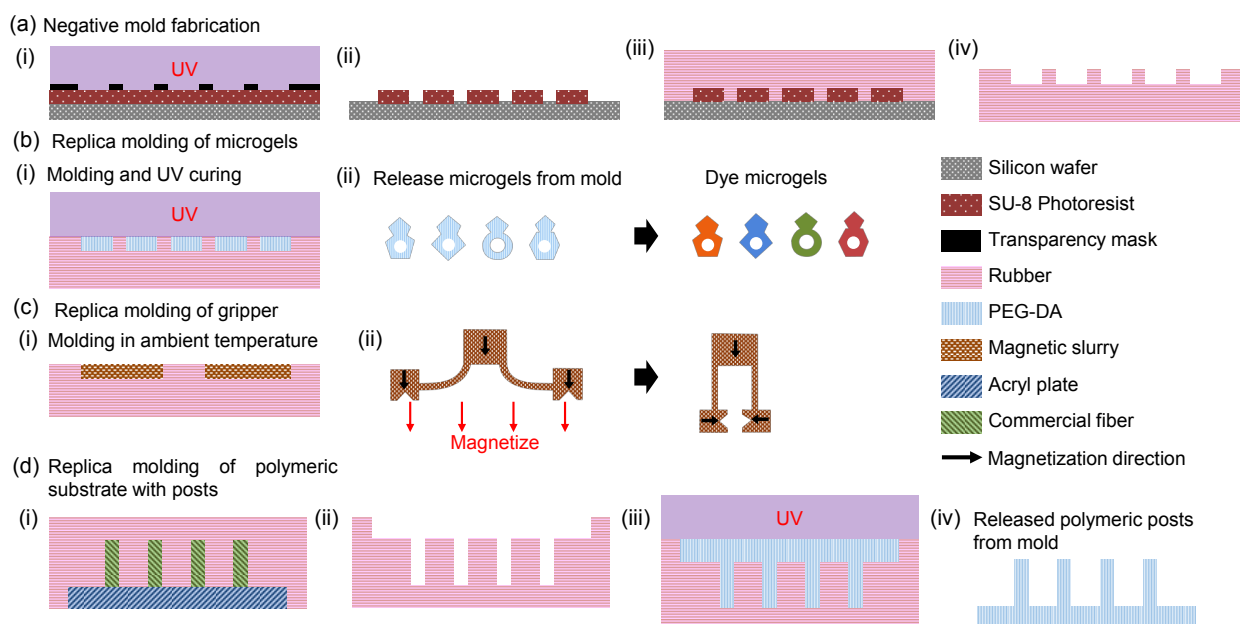


Figure 2. Fabrication process. (a) Negative mold fabrication. (i) Photolithography to fabricate positive mold of components. SU-8 photoresist layer coated on a silicon wafer was exposed to ultraviolet (UV) light through transparency mask with target patterns. (ii) Developed positive mold. (iii) Rubber was casted over the positive mold. (iv) Negative rubber mold with target patterns. (b) Replica molding of microgels. (i) PEG-DA oligomer was poured into negative mold and exposed to UV light to cure the microgels. (ii) Photopolymerized microgels were released from the mold and dyed in each different colour. (c) Replica molding of buoyant microgripper. (i) Magnetic slurry was poured into negative mold and cured under ambient temperature. Magnetic slurry contained polyurethane, magnetic microparticles, and hollow glass beads. (ii) Released component from the mold was deflected and then magnetized. In relaxed state, each part had different magnetization directions. (d) Replica molding of polymeric substrate with posts. (i) Commercial fibers were attached to the acryl plate. Rubber was casted over the mold. (ii) Negative rubber mold. (iii) PEG-DA oligomer was poured into negative mold and exposed to UV light to cure the structure. (iv) Posts attached polymeric substrate was released from the mold.

Microgels were fabricated by molding poly(ethylene glycol) diacrylate (PEG-DA), ultraviolet (UV) curing, and dyeing with

different recognizable colours (Figure 2(b)). Similar to the microgel fabrication process, the gripper was also molded but

with ambient temperature curing. The gripper was made of composite magnetic materials, which consisted of soft elastomeric polyurethane mixed with magnetic microparticles for actuation, and hollow glass microbeads for ease of levitation of the gripper by reducing the density of the robot. The cured gripper was magnetized while beams were deformed to 90 degrees (Figure 2(c)(ii)). To make polymeric substrate with posts, we first fabricated a negative rubber mold by casting silicon rubber over fibers attached to an acrylic plate (Figure 2(d)(i)). The rest of the procedure was similar to the microgel replica molding and UV curing process.

Figure 3 shows the fabricated microgels and polymeric substrate with posts, which were used for 3D heterogeneous microgel assembly. Each microgel had a center hole with 400  $\mu\text{m}$  diameter and a protruded square-shaped part at one end of the microgel as a handle. The contrary square-shaped gripping magnets of the microgripper grabbed the square-shaped handle with a maximized contact area due to shape-matching designs. Thus, microgels were tightly grabbed during 3D transportation and assembly process. In addition, microgels were individually identifiable by their 2D shapes, such as circle, triangle, square, or hexagonal shapes, and colours, such as red, brown, violet, green, or blue, to show a heterogeneity of the assembly. Colour-coded microgels were made by absorbing dyes with different colours to the microgels. The different colours in the experiments conceivably represent a broad range of materials, such as different living cells.

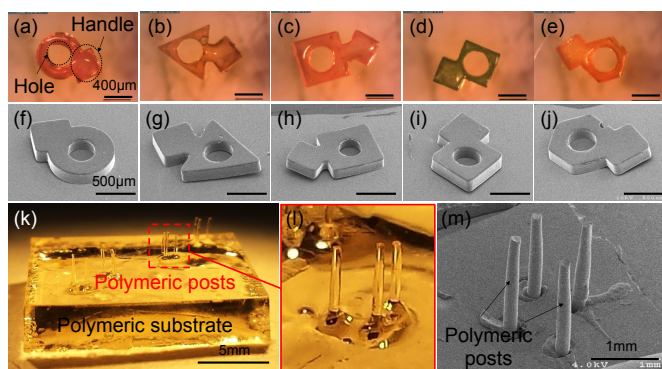


Figure 3. Fabricated features. (a)-(e) Fabricated PEG-DA microgel samples. Each microgel had a centre hole and a handle for gripping. During assembly process, the hole of the microgel was aligned on top of the post. (a) Violet circular-shaped microgel. (b) Brown inverted triangular-shaped microgel. (c) Red square-shaped microgel. (d) Green rotated square-shaped microgel. (e) Yellow hexagonal-shaped microgel. Scale bars, 400  $\mu\text{m}$ . (f)-(j) Scanning electron microscope (SEM) images of fabricated microgels in (a)-(e), respectively. Scale bars, 500  $\mu\text{m}$ . (k) Polymeric substrate with posts. (l) Magnified image of three posts on the substrate in (k). (m) A SEM image of four polymeric posts on the substrate.

If cell-encapsulated microgels are constructed in 3D, cells inside a unit microgel block would proliferate and interact with adjacent cells enabling formation of tissues as parts of living organs depending on the type of containing cells. To closely mimic the environments, we used a biocompatible polymer, PEG-DA, to fabricate both microgel blocks and polymeric posts. In addition, when the cells will be encapsulated in microgels, the size of each microgel should be defined in terms of the diffusion limit of nutrients to avoid cell starvation in the absence of vascularization. Therefore, we fixed the thickness of all the microgels in Figures 3(a)-(e) to 180  $\mu\text{m}$ . These microgel conditions were chosen to demonstrate our technique is

applicable to 3D assembly of cell-encapsulated microgels. These microgels fabricated in Figure 3(a)-(e) were assembled on polymeric posts shown in Figure 3(k)-(m).

Since both microgels and polymeric posts were made of the same biocompatible materials, the posts did not need to be removed after assembly and could function as a scaffold with microgels. Each polymeric post had a diameter of 200  $\mu\text{m}$  and heights of 1.5-2 mm. Since the polymeric substrate with posts was molded from a single negative rubber mold, all the posts and substrate were connected and made out of the same material. For complex assembly of microgels in a 3D shape, multiple posts were fabricated in a single assembly site. The maximum number of layers assembled on a single post depended on the height of the post. The thickness of each microgel was about 180  $\mu\text{m}$ ; so, a maximum of 8-11 microgels could be assembled on a single post with 1.5-2 mm height. Since microgels were molded out of the negative mold which was cast over photoresist patterns as explained in the Materials and Methods section, the thickness of each microgel was determined by the thickness of the coated photoresist. Therefore, the uniformity of coated photoresist on the substrate mainly affects the uniformity of thickness of microgels.

### Pick-and-place 3D robotic microgel assembly

For a proof-of-concept demonstration of pick-and-place 3D robotic microgel assembly with remotely controlled microgripper, we showed the full procedure from gripping to assembling microgels on a single post in Figure 4 (Supplementary Information video S1 shows the zoomed-in process of gripping microgel, and zoomed-out 3D motion control). Figure 4(a) shows the schematic demonstration of the pick-and-place process using a microgripper and Figures 4(b)-(f) show time-lapse images of this process. Top and bottom images in Figures 4(b)-(f) correspond to the  $x$ - $y$  plane top microscope view and the corresponding  $y$ - $z$  plane side microscope view of the objects, respectively. Here, the microgel-holding gripper moved its position to the target site in the top view image sequences, and it moved up or down in the side view image sequences. Initially, microgels and the magnetic microgripper were put on the substrate in a water-filled enclosed container with a 20 mm  $\times$  20 mm  $\times$  20 mm working space. Therefore, all the assembly process illustrated in Figure 4(a) took place in this enclosed workspace. The microgripper was tele-operated using a joystick to grip the microgel on the substrate. The gripper moved to a nearby location of the target microgel with stick-slip or rolling motion and aligned its gripping magnets to the handle position of the microgel. By applying a constant magnetic field, the gripping magnets were opened. After aligning the magnets with the handle part of the microgel, the magnetic field was reduced to tightly grip the microgel (Figure 4(b)). The microgel-holding microgripper was then levitated by applying a magnetic gradient pulling force to transport the microgel for 3D control in the aquatic environment (Figure 4(c)). The position of the gripper was detected and the gripper was tele-operated to move to the target position denoted as a small green cross in the top view and a green horizontal line in the side view (Figure 4(d)). When the hole of the microgel gripped by the microgripper was aligned with the top position of the target post, the gripper moved downward to assemble the microgel on the post (Figure 4(e)). Then, the gripping magnets of the gripper were opened again to release the microgel by applying a constant magnetic field (Figure 4(f)). This simple pick-and-place strategy allowed the microgripper to stack microgels to a desired number of

layers with heterogeneity. By repeating the process, microgels were assembled up to seven layers in a vertical direction on the single post as shown in Figures 4(g)-(h). The number of layers stacked on the post depends on the height of the post, which could be controlled during the fabrication process as shown in Figure 2(d)-(i). This height of the post could be increased to assemble more microgel layers. Supplementary Information video S2 shows the process of multi-layer assembly of microgels up to ten layers. The mobile microgripper was

capable of assembling complex heterogeneous systems with a lot of layers by individually controlling not only the position of each microgel during the assembly process, but also the type of the microgel and the number of layers to get necessary heterogeneous 3D structure within enclosed aquatic environments. Therefore, our microrobot assembly method could have a potential for broader applications in a construction of complex 3D heterogeneous systems.

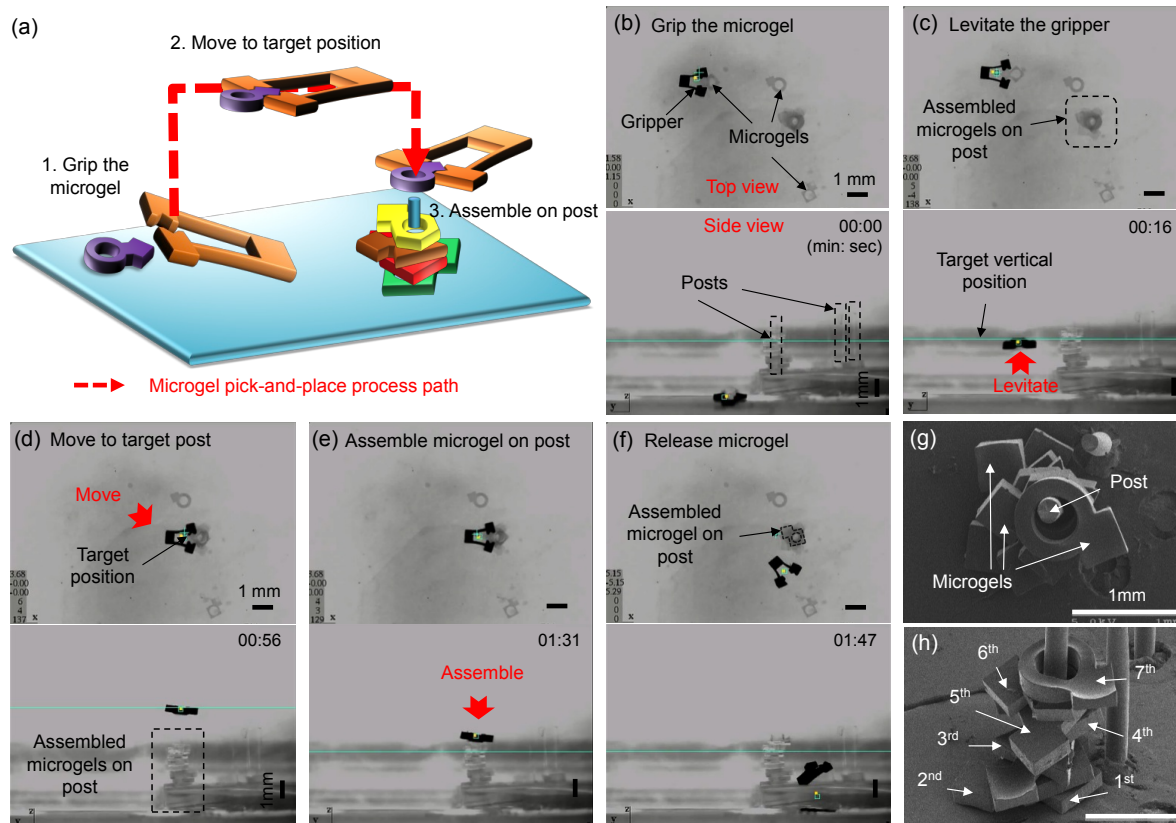


Figure 4. Proof-of-concept demonstration of the microgel pick-and-place on the polymeric post using remotely controlled magnetic microgripper. (a) Schematic diagram of pick-and-place process. First, microgripper gripped the microgel on the substrate by magnetically controlling in 2D. Then, microgel-gripping robot levitated and moved to the target assembly position. Finally, the gripper moved down by assembling the microgel on the post. (b)-(f) Time-lapse images of the pick-and-place process. Top images show the top microscope views in x-y plane and bottom images show the side microscope views in y-z plane. (b) Microgripper moved to nearby location of target microgel with stick-slip locomotion, and aligned gripping magnets with the handle the microgel. By applying constant magnetic field, gripping magnets were opened. Then, while reducing the magnetic field, the gripping magnets started to tightly grip the handle of the microgel. (c) The microgel-gripping microgripper was levitated by applying magnetic gradient pulling force. The position of the gripper was detected and the gripper was tele-operated to move to the target position denoted as a small green cross with a solid square spot in the top view and a green horizontal line in the side view. (d) The hole of the microgel was aligned with the top position of the post. (e) The gripper moved down and assembled the microgel on the post. (f) By applying constant magnetic field, gripping magnets were opened again to release the microgel. (g)-(h) SEM images of stacked microgels on the single post. Scale bars, 1 mm. (g) Top image. (h) 3D view image. Seven different microgels were assembled on the single post by simply repeating the pick-and-place process using magnetic microgripper.

### Heterogeneous 3D microrobotic microgel assembly

The mobile microgripper allowed building a variety of 3D geometries with different shapes and colours of microgels by taking advantage of prefabricated posts. This capability could be critical for tissue engineering, where small building blocks with certain types of cells inside form appropriate shapes to

advance into any tissue units in 3D. Since the gripper was capable of moving in all directions during gripping or releasing process, the orientation and position of microgels were dynamically controlled and adjusted while building a variety of complex systems.

## ARTICLE

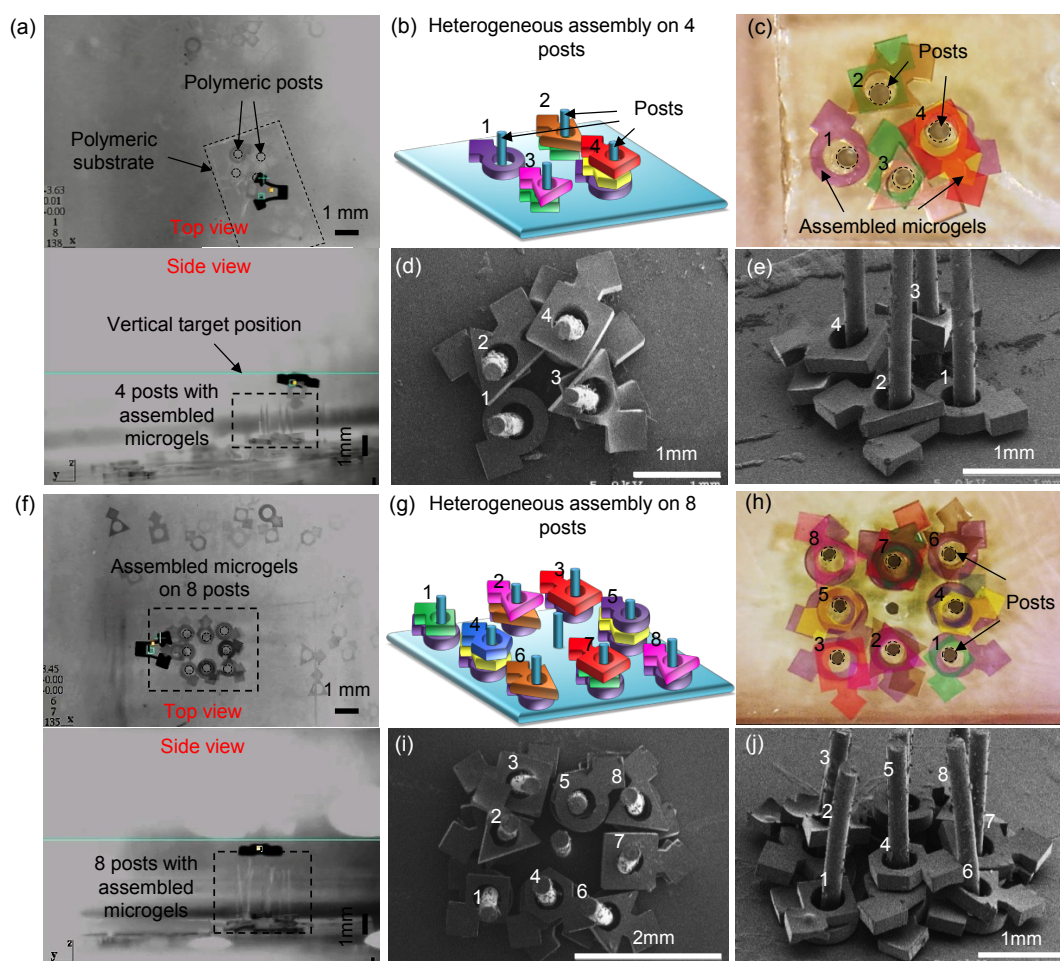


Figure 5. Complex heterogeneous 3D microrobotic assembly of various microgels on multiple posts. Assembly process was scalable to construct complex heterogeneous structures with multiple posts. (a) Heterogeneous 3D assembly of microgels on four different posts using mobile microgripper. Polymeric posts and substrate are denoted as black dash circles and box, respectively. Top microscope image shows the top view ( $x$ - $y$  plane) of the microgel-holding microgripper aligning to the target post. Bottom microscope image shows the corresponding side view ( $y$ - $z$  plane) of the top image. Various microgels were assembled on four different posts and microgel-holding microgripper was levitated up to the vertical target position. (b) Schematic illustration of heterogeneously assembled microgels on four different posts. Total eight microgels with six different types were used in the experiments. Each code of microgel was represented as a shape and colour. One microgel on post 1, two different microgels on both posts 2 and 3, and three different microgels on post 4 were assembled, respectively. (c) Top microscope image of assembled microgels as illustrated in (b). Black-dashed circles are four different polymeric posts on the substrate. (d)-(e) SEM images of heterogeneously assembled microgels on four different posts. White numbers on images correspond to the number of posts from (b). (d) Top image. (e) 3D view image. (f) Heterogeneous 3D assembly of microgels on eight different posts using mobile microgripper. Top image shows the top view ( $x$ - $y$  plane) of the microgel-holding microgripper aligning to the target post. Black-dashed box is the region with assembled microgels on eight posts. Bottom image shows the corresponding side view ( $y$ - $z$  plane) of the top image. Various microgels were assembled on eight different posts and microgel-holding microgripper was levitated up to the vertical target position. (g) Schematic illustration of heterogeneously assembled microgels on eight different posts. Total twenty different microgels with seven different types were assembled on eight different posts. Two microgels on posts 1, 3, 6, and 8, and three different microgels on posts 2, 4, 5, and 7 were assembled, respectively. Each microgel has different shape and colour code. (h) Top microscope image of assembled microgels as illustrated in (g). Black-dashed circles are eight different polymeric posts on the substrate. (i)-(j) SEM images of heterogeneously assembled microgels on eight different posts. White numbers on images correspond to the number of posts from (g).

A scalability of our microrobotic pick-and-place assembly method is demonstrated as heterogeneous 3D microgel assemblies on multiple posts as shown in Figure 5. On nearby positioned several polymeric posts, microgels with each different shape and colour code were heterogeneously

assembled by the microgripper showing a complexity and variety of the assembly. Figure 5(a) shows robotic heterogeneous assembly of microgels in four different posts. The top microscope image in Figure 5(a) shows the top view ( $x$ - $y$  plane) of the microgel-holding microgripper aligning to the

target post, and the bottom image shows the corresponding side view ( $y$ - $z$  plane) of the top image.

Various microgels were assembled on four different posts and the microgel-holding mobile microgripper was levitated up to the vertical target position. All the microgels were sequentially tele-operated to flexibly assemble them to the preplanned order of stacks on the posts. The schematic illustration in Figure 5(b) shows the constructed microsystem composed of eight different microgels on four posts. The type and number of microgels assembled on each post were controlled during assembly. One microgel on post 1, two microgels on both posts 2 and 3, and three microgels on post 4 were assembled showing increasing height of constructs. Figure 5(c) shows the top microscope view of final 3D constructs as illustrated in Figure 5(b). Corresponding SEM image in Figure 5(d)-(e) show that different shape-coded microgels were heterogeneously assembled on four different posts. Figure 5(f) shows a large size of complex heterogeneous 3D assembly of microgels on eight different posts to demonstrate a scalability of our method (Supplementary Information video S3 shows heterogeneous 3D assembly process on eight different posts). Total twenty microgels with seven different types were assembled on eight posts as shown in schematic illustration of Figure 5(g). Each type is represented by the shape and colour of the microgel. Since coloured microgels contained different colour dyes, different colours in these experiments may represent a broad range of materials, such as organic or inorganic beads, living cells, nanoparticles, and other different materials. Therefore, heterogeneously assembled microgels with seven different colours in Figure 5(h) represent seven different types of materials contained in a single 3D complex system. In addition, these structures were easily fixed together with the assistance of posts during the assembly process. Therefore, the created 3D assembled structures were stable without any secondary crosslinking steps even in aquatic environments with possible liquid flows. In addition, the microgripper controlled the orientation of microgels by positioning their handles pointing to outward directions during the assembly to reduce interference between microgels as shown in Figure 5(i) and Supplementary Information video S3. The interference between microgels can be reduced by properly increasing the space between posts or by using shape-matching microgels like a jigsaw puzzle to eliminate creakiness due to unnecessary gaps between microgels.

## Materials and Methods

**Coded microgel fabrication.** The coded microgels were fabricated by a replica molding technique. The mold was prepared using standard photolithography. For the photolithography process, SU-8 2050 photoresist (MicroChem) was first spin-coated on a silicon wafer at 1000 rpm velocity for 30 seconds (approximately 180  $\mu\text{m}$  of SU-8 2050 photoresist thickness). It was soft baked for 7 minutes at 65°C, and then for 45 minutes at 95°C on a hotplate. Second spin-coating on the baked wafer was executed again for higher thickness of microgels. The second coating condition was 3000 rpm velocity for 30 seconds, which made total 180  $\mu\text{m}$  of photoresist thickness. After soft baking for 3 minutes at 65°C, and then for 9 minutes at 95°C on a hotplate, features for ring-shaped microgels were patterned through a film photomask (designed by AUTOCAD) of 20,000 dpi resolution and post baked for 5 minutes at 65°C, and then for 15 minutes at 95°C on a hotplate. The patterned wafer was then developed for 15 minutes in SU-8 developer (MicroChem). Silicon rubber compound (MoldMax Series, Smooth-on) was cast over developed SU-8 positive features on the wafer. On the replica

negative mold, poly(ethylene glycol) diacrylate (MN=700, Sigma-Aldrich) with 15% 2, 2-Dimethoxy-2-Phenylacetophenone, 99% photoinitiator (Sigma-Aldrich) was molded and photopolymerized by ultraviolet (UV) curing for 2 minutes. Coloured dye materials were absorbed into released microgels from the mold by dipping the microgels in corresponding dye solution for 1 hour. Shape codes of microgels were determined by the design of microgels during photolithography process, and colour codes of microgels were determined by the colours during dyeing process.

**Magnetic microgripper fabrication.** The microgripper was fabricated by standard photolithography and replica molding techniques. The replica negative mold for microgrippers was fabricated by the same process with coded microgel fabrication. During the photolithography step, the thickness of microgripper pattern was controlled to be about 300  $\mu\text{m}$ . On the replica rubber mold, magnetic slurry composed of polyurethane (ST-1087, BJB Enterprises), magnetic microparticles of average 5  $\mu\text{m}$  diameter (MQFP-15-7, Magnequench), and hollow glass microbeads of average 65  $\mu\text{m}$  diameter (3M Glass Bubbles K1) with 20:10:1 weight ratio was molded for 24 hours. The densities of polyurethane, magnetic microparticles, and hollow glass microbeads were 1.08, 7.61, and 0.125  $\text{g}/\text{m}^3$ , respectively, and the mixture weight ratio was controlled to achieve the final density of microgripper to be 1.2  $\text{g}/\text{m}^3$  for an ease of levitation by the magnetic gradient pulling force. The mixture was cured under ambient temperature for 18 hours. The cured microgripper was released from the mold and magnetized under 1 Tesla constant magnetic field while beams were deformed to 90 degrees. After magnetization, beams were relaxed to initial gripper shape. The beam length and width of the gripper used in the experiments were 700  $\mu\text{m}$  and 70  $\mu\text{m}$ , respectively, and the magnetization was 3.138 memu.

**Polymer micropost fabrication.** The polymeric substrate with microposts was also fabricated by the replica molding technique. The positive mold of the posts was made by laser cutting circular shapes on acryl plate, fixing ends of commercial thin fibers (diameter = 200  $\mu\text{m}$ , length = 5 mm Trilene) to the circular holes, and bonding the fibers to holes in acryl plate with a glue. The silicon rubber was then cast over the positive acryl plate mold. PEG-DA with photoinitiator was also molded into the negative rubber mold. For the compatibility between microgels and posts, we used same materials for both ring-shaped coded microgels and polymeric substrate with posts. The mold with PEG-DA was degassed for 15 minutes to fill polymers in thin and long holes for post structures, and exposed to UV light for 3 minutes to photopolymerize PEG-DA. The cured polymeric substrate with posts was gently released from the mold. The substrate with posts was cleaned by dipping it in ethyl alcohol for 24 hours and stored in DI water. Posts were dyed with colours to recognize the position during experiments.

**Three-dimensional magnetic actuation and motion control.** The microgripper was actuated and controlled by a customized electromagnetic coil system with eight coils arranged pointing to a common center point.<sup>[19-20]</sup> A magnetic field and its spatial gradient were supplied by controlling running currents through electromagnetic coils using a PC with data acquisition system using linear electronic amplifiers (Dimension Engineering Inc., SyRen 25) with feedback from Hall-effect current sensors (Allegro Microsystems Inc., ACS714). The magnetic torques

and gradient pulling forces under an external magnetic field  $B$  could be obtained by the following original equations

$$T_m = V_m(m \times B) \quad (1)$$

$$F = V_m(m \cdot \nabla)B \quad (2)$$

where  $V_m$  and  $m$  are the volume and the magnetization of the magnetic part, respectively. The position of the microgripper was detected using two grayscale CCD cameras (Foculus) simultaneously and processed by morphological algorithms in OpenCV library. A Kalman filter was also implemented to reduce the noise of visual tracking. The resolution of detection was within 1-2 pixels ( $\sim 100 \mu\text{m}$ ). Thus, the precision of the part assembly in  $x$ - and  $y$ -direction is around  $200 \mu\text{m}$ , which is limited by the visual detection precision with the given constant optical zoom of our setup. The  $x$ - $y$  precision of the assembly process will be improved by increasing the optical imaging resolution using an active variable optical zooming setup in the future, which could also actively change the imaged workspace area.

A PID feedback controller together with a feedforward controller was used to minimize the error between a 3D position of the microgripper and the reference input. The feedforward term needs to be recalibrated when the microgripper grabs a new microgel, which may degrade the position control performance in  $z$ -direction. The resolution of visual detection also limits the performance of position control. These limitations could be overcome by designing a feedback control system using high-resolution  $z$ -position visual feedback. In this work, the gripper was controlled to move to the target position with errors less than half of the body width ( $\sim 200 \mu\text{m}$ ). Under different poses of the microgripper while moving in 3D, different parameters of the controller were pretuned and scheduled to deal with orientation-dependent dynamics. Thus the gripper could be levitated with different poses for the assembly in various orientations.

The degree-of-freedom along the body axis of the gripper could not be precisely controlled without using full body orientation feedback but could be roughly changed by slightly modifying the orientation of the applied magnetic field, which did not cause any issue for 3D assembly of microgels during the experiments.

**Modification of microscope images.** For clarity, images acquired by microscope were modified in Figure 5(c) and Figure 5(h). Since microgels were dyed very lightly compared to the gripper to eliminate interferences during the gripper detection process, same artificial colours used for dye absorption into microgels in the experiments were added to the image of microgels using Adobe Photoshop.

## Discussions

Since the microgripper pick-and-places each microgel individually, this serial assembly method takes much more time than parallel assembly methods such as self-assembly. Although it is a slow serial process currently, the proposed method enables complex asymmetric 3D constructs, high assembly yield, and high flexibility in component choice with compared to self-assembly. Such assembly speed issue could be improved using two approaches as a future work. First, a team of microrobots can assemble 3D constructs in parallel using smart magnetic materials<sup>21-25</sup> and advanced control and actuation methods.<sup>26-30</sup> Next, automating the pick-and-place assembly process, the operation time could be dramatically reduced. In current proof-of-concept study, the gripper was teleoperated using a joystick by a user directly to grip the microgel on the substrate using camera image feedback. This

step takes significant processing time, which will be reduced significantly by vision-based automatic control.<sup>16</sup>

Assembled microgels were mechanically stable during the assembly process without any secondary cross-linking steps even in aquatic environments with possible liquid flows or other external disturbances, because the polymeric posts were used to fix each microgel block during and after the assembly. Therefore, assembled microgels did not move away from the target position or collapse after the assembly.

Our experimental conditions such as materials, size of components, and experimental setup are selected towards tissue engineering applications. Biocompatible microgels undergo degradation to be used as tissue scaffold materials in the future. But environmental conditions such as pH, temperature, chemicals, and light irradiation time could affect the gel degradation behaviour, and need to be customized for controlled degradation behavior.

For future *in vivo* biomedical applications, the environmental conditions and gripper properties need to be selected carefully. The material of the microgripper should be biocompatible like microgels and microposts. Current microgripper contains magnetic particles, glass hollow microbeads, and polyurethane, and such material compositions need to be modified to be biocompatible or grippers should be coated by parylene type of biocompatible conformal coatings for *in vivo* applications. Furthermore, design parameters of the microgripper and microgels such as shape and size of gripper tip endings and microgels need to be customized for a given specific application where magnetic actuation capability also changes according to the dimensions and material composition of the microgripper.

## Conclusions

In this study, we have presented heterogeneous 3D structure construction by assembling differently coded microgels using an untethered mobile microgripper controlled by an external electromagnetic coil system. The whole assembly process took place inside an enclosed aquatic environment. Previously, all 3D microgel assemblies were constructed by self-assembly methods, which were hard to control the number of microgel layers, and previous robotic assembly methods had limitations on the maximum number of layers in the assembly. In contrast, the proposed pick-and-place assembly method by an untethered mobile magnetic microgripper demonstrated a precise assembly of complex 3D structures by individually controlling the position and orientation of the microgel. Microgels coded with different shapes and colours were heterogeneously assembled up to ten layers in aquatic environments. We envision that pick-and-place robotic heterogeneous 3D assembly technique would not only impact current microgel assembly based potential tissue engineering construct applications with its flexibility, precision, and versatility, but also enable 3D additive manufacturing of heterogeneous components in a wide range of application areas such as flexible electronics, bioengineering, optical microdevices, and electronic packaging in the future.

## Acknowledgements

The authors thank J. Giltinan and E. Diller for initial assistance with electromagnetic coil system. This work is supported by the National Science Foundation, National Robotics Initiative program under NRI-1317477 grant number. Any opinions, findings, and conclusions or recommendations expressed in this

material are those of the authors and do not necessarily reflect the views of the National Science Foundation.

## Notes and references

<sup>a</sup> Carnegie Mellon University, 5000 Forbes Avenue, Pittsburgh, PA 15213, USA

<sup>b</sup> Max Planck Institute for Intelligent Systems, Heisenbergstr. 3, 70569 Stuttgart, Germany

† Equally contributing authors

Electronic Supplementary Information (ESI) available: [Theoretical analysis, supporting results, SI Figure S1-S5, Video S1-S3]. See DOI: 10.1039/b000000x/

1. D. Seliktar, *Science*, 2012, **336**, 1124-1128.
2. C. M. Hwang, S. Sant, M. Masaali, N. N. Kachouie, B. Zamanian, S.-H. Lee, A. Khademhosseini, *Biofabrication*, 2010, **2**, 035003.
3. T. Lu, Y. Li, T. Chen, *International Journal of Nanomedicine*, 2013, **8**, 337-350.
4. S. Kim, F. Qiu, S. Kim, A. Ghanbari, C. Moon, L. Zhang, B. J. Nelson, H. Choi, *Advanced Materials*, 2013, **25**, 5863-5868.
5. Y. Du, E. Lo, S. Ali, A. Khademhosseini, *Proceedings of the National Academy of Sciences USA*, 2008, **105**, 9522-9527.
6. Y. Du, M. Ghodousi, E. Lo, M. K. Vidula, O. Emiroglu, A. Khademhosseini, *Biotechnology and Bioengineering*, 2010, **105**, 655-662.
7. S. E. Chung, Y. Jung, S. Kwon, *Small*, 2011, **7**, 796-803.
8. T. Yue, M. Nakajima, M. Takeuchi, C. Hu, Q. Huang, T. Fukuda, *Lab on a Chip*, 2014, **14**, 1151-1161.
9. Y. L. Han, Y. Yang, S. Liu, J. Wu, Y. Chen, T. J. Lu, F. Xu, *Biofabrication*, 2013, **5**, 035004.
10. F. Xu, T. D. Finley, M. Turkyaydin, Y. Sung, U. A. Gurkan, A. S. Yavuz, R. O. Guldiken, U. Demirci, *Biomaterials*, 2011, **32**, 7847-7855.
11. F. Xu, C.-A. M. Wu, V. Rengarajan, T. D. Finley, H. O. Keles, Y. Sung, B. Li, U. A. Gurkan, U. Demirci, *Advanced Materials*, 2011, **23**, 4254-4260.
12. S. Tasoglu, C. H. Yu, H. I. Gungordu, S. Guven, T. Vural, U. Demirci, *Nat Commun*, 2014, **5**, 1-11.
13. H. Wang, Q. Shi, T. Yue, M. Nakajima, M. Takeuchi, Q. Huang, T. Fukuda, *International Journal of Advanced Robotic Systems*, 2014, **11**, 1-12.
14. Y. Du, M. Ghodousi, H. Qi, N. Haas, W. Xiao, A. Khademhosseini, *Biotechnology and Bioengineering*, 2011, **108**, 1693-1703.
15. C. Pawashe, S. Floyd, M. Sitti, *International Journal of Robotics Research*, 2009, **28**, 1077-1094.
16. C. Pawashe, S. Floyd, E. Diller, M. Sitti, *IEEE Transactions on Robotics*, 2012, **28**, 467-477.
17. Z. Ye, E. Diller, M. Sitti, *Journal of Applied Physics*, 2012, **112**, 064912.
18. E. Diller, M. Sitti, *Foundations and Trends in Robotics*, 2013, **2**, 143-259.
19. S. Tasoglu, E. Diller, S. Guven, M. Sitti, U. Demirci, *Nat Commun*, 2014, **5**, 1-9.
20. E. Diller, M. Sitti, *Advanced Functional Materials*, 2014, **24**, 4397-4404.
21. E. Diller, S. Miyashita, M. Sitti, *RSC Advances*, 2012, **2**, 3850-3856.
22. E. Diller, J. Zhuang, G. Z. Lum, M. R. Edwards, M. Sitti, *Applied Physics Letters*, 2014, **104**, 174101.
24. E. Diller, N. Zhang, M. Sitti, *Journal of Micro-Bio Robotics*, 2013, **8**, 121-131.
25. S. Miyashita, E. Diller, M. Sitti, *International Journal of Robotics Research*, 2013, **32**, pp. 591-613.
26. E. Diller, J. Giltinan, M. Sitti, *International Journal of Robotics Research*, 2013, **32**, 614-631.
27. E. Diller, S. Floyd, C. Pawashe, M. Sitti, *IEEE Trans. on Robotics*, 2012, **28**, 172-182.
28. E. Diller, C. Pawashe, S. Floyd, M. Sitti, "International Journal of Robotics Research", 2011, **30**, 1667-1680.
29. S. Floyd, E. Diller, C. Pawashe, M. Sitti, *International Journal of Robotics Research*, 2011, **30**, 1553-1565.
30. C. Pawashe, S. Floyd, M. Sitti, *Applied Physics Letters*, 2009, **94**, 161408.